A General Constitutive Model for Vascular Tissue Considering Stress Driven Growth and Biological Availability

F. J. Bellomo[1], S. Oller[2], F. Armero[3] and L. G. Nallim[1]

Abstract: Some of the key factors that regulate growth and remodeling of tissues are fundamentally mechanical. However, it is important to take into account the role of biological availability to generate new tissue together with the stresses and strains in the processes of natural or pathological growth. In this sense, the model presented in this work is oriented to describe growth of vascular tissue under "stress driven growth" considering biological availability of the organism. The general theoretical framework is given by a kinematic formulation in large strain combined with the thermodynamic basis of open systems. The formulation uses a multiplicative decomposition of deformation gradient, splitting it in a growth part and visco-elastic part. The strains due to growth are incompatible and are controlled by unbalanced stresses related to a homeostatic state. Growth implies a volume change with an increase of mass maintaining constant the density. One of the most interesting features of the proposed model is the generation of new tissue taking into account the contribution of mass to the system controlled through the biological availability. Because soft biological tissues in general have a hierarchical structure with several components (usually a soft matrix reinforced with collagen fibers), the developed growth model is suitable for the growth characterization of each component. This allows considering a different behavior for each of them in the context of a generalized theory of mixtures.

Keywords: Cardiovascular tissue, Growth, Atrophy, Biological availability.

[1] INIQUI – CONICET. National University of Salta, Av. Bolivia 5150, 4400 Salta, Argentina.

[2] CIMNE. International Center for Numerical Method in Engineering (http://www.cimne.com/). UPC, Technical University of Catalonia (Barcelona Tech. http://www.upc.edu/eng/), Jordi Girona 1-3, 08034 Barcelona, Spain.

[3] Department of Civil and Environmental Engineering University of California, Berkeley, USA

1   Introduction

Since the formulation of the first continuum growth model, called "Adaptive Elasticity Theory", published more than a quarter century by Cowin and Hegedus (1976), the modeling and simulation of biomechanical processes have been growing in interest. Biomaterials like hard and soft tissues show the ability to adapt their external shapes and internal microstructures as an active response to environmental changes.

The theory of adaptive elasticity (Cowin and Hegedus 1976) considers the biological structure as an open system which allows a constant exchange of mass, momentum, energy and entropy with the surrounding environment. There are other models, such as Epstein and Maugin (2000) that allows exchanges in terms of mass flows. These flows are typically attributed to the migration of cells resulting from a source of mass due to growth, contraction, death, division or cell enlargement.

Soft tissue modeling requires a geometric description based on a nonlinear kinematics to address the consideration of large strains (Rodriguez et al. 1994, Cowin 1996, Holzapfel and Ogden 2003, Gasser and Holzapfel 2002). Laboratory tests show that many biological soft tissues are incompressible or nearly incompressible when subjected to large strains and the material exhibits a strong viscous behavior (Fung 1996).

The general formulation presented in this paper consists of two main developments. First, a mechanical model based on previous formulations of mixing theories (Car et al. 2000, 2001, Oller et al. 2003, Rastellini et al. 2008, Martinez et al. 2011) is proposed. The basic concepts of these theories are extended here to take into consideration general behaviors, such as generalized large strains framework including kinematics and compatibility equations for serial-parallel behavior. Particularly, arterial tissue can be modeled as an isotropic soft matrix reinforced with preferentially oriented collagen fibers. Secondly, for each component of the tissue, a growth model considering the biological availability is proposed. The reason of this consideration is that the mechanical stimulus is not the only necessary factor to produce a mass change; the biological field is also involved. Metabolism must be able to generate new tissue in response to stimulus. In this aspect, the main contribution of this work is the formulation and the computational implementation of the coupling between mechanical and biological fields. This is achieved considering the biological availability for growth by means of a proposed internal variable θ. The evolution of θ results from the balance between the nutrients contributed to the system and those already used in tissue growth; following the general idea developed by the authors (Bellomo el al. 2011).

Finally, to illustrate the general formulation presented in this article, two numerical examples are presented. The first example considers growth during the stretching

of a single element along two different fiber orientations to address the capability of the model to capture the fiber induced anisotropy of the tissue. The second example examines the effect of the nutrients intake distribution in the growth pattern of a single component along a notched tissue patch.

2 Constitutive model: A mixing theory for the behavior of biological materials

2.1 Generalized rule of mixtures for small strains

The general mechanical framework of this work is a new formulation based on an extension of the generalized rule of mixtures proposed by Car et al. (2000) (more detail about this formulation can be found in the following references Car et al. 2000, 2001, Oller et al. 2003, Rastellini et al. 2008, Martinez et al. 2011). This theory allows studying the behavior of composite materials as a combination of individual components with its own constitutive law, each one satisfying appropriate serial-parallel compatibility equations. These equations establish the interaction kinematics conditions between the components of the composite material. The total composite strain decomposition in each material component for the linear and small strain case is introduced throughout the following proposed expression,

$$\boldsymbol{\varepsilon}_c = [(1 - \chi_c)\,\mathbf{I}\boldsymbol{\varepsilon} + \chi_c\,\boldsymbol{\phi}_c\boldsymbol{\varepsilon}] \tag{1}$$

where the subscript c refers to c-th component, $\mathbf{I}$ is the fourth order identity tensor, $\boldsymbol{\varepsilon}_c$ is the strain tensor of the c–th component, $\boldsymbol{\varepsilon}$ is the strain tensor of the composite, χ_c is the serial-parallel coupling parameter that depends of the angle between the fiber and the principal stress direction and $\boldsymbol{\phi}_c$ establishes the strain of the c–th component when all the components are working in serial.

Eq. 1 can also be written as:

$$\boldsymbol{\varepsilon}_c = [(1 - \chi_c)\,\mathbf{I}_4 + \chi_c\boldsymbol{\phi}_c] : \boldsymbol{\varepsilon} \tag{2}$$

The expression for $\boldsymbol{\phi}_c$ is derived as follows:

$$\boldsymbol{\varepsilon} = \sum_{c=1}^{n} k_c \boldsymbol{\varepsilon}_c = \sum_{c=1}^{n} k_c \mathbf{C}_c^{-1} : \boldsymbol{\sigma}_c = \sum_{c=1}^{n} k_c \underbrace{\mathbf{C}_c^{-1} : \mathbf{C}^{ser}}_{\boldsymbol{\phi}_c} : \boldsymbol{\varepsilon} \tag{3}$$

where $k_c = d\mathrm{v}_c/d\mathrm{v}$ is the volumetric participation ratio of each component (v_c is the c–th component volume and v is the total volume), $\mathbf{C}_c$ is the c–th component constitutive tensor and $\mathbf{C}^{ser} = \left[\sum_{c=1}^{n} k_c \mathbf{C}_c^{-1}\right]^{-1}$ is the composite constitutive tensor with its n components working in series.

2.2 Generalized rule of mixtures for finite strains

The free energy in the reference configuration is given by

$$m\Psi = \sum_{c=1}^{n} m_c k_c \Psi_c \tag{4}$$

where m and m_c are, respectively, the composite and the c–th component mass, Ψ and Ψ_c are the composite and the c–th component free energy respectively.

Similarly to the small strains case the Green-Lagrange strain tensor of the c–th component on the reference configuration is given by

$$\mathbf{E}_c = [(1 - \chi_c)\mathbf{I}_4 + \chi_c \boldsymbol{\phi}_c] : E \tag{5}$$

where $\mathbf{E}$ is the composite Green-Lagrange strain tensor.

Also, similarly to the small strains case (see Eq. 3) the serial behavior tensor $\boldsymbol{\phi}_c$ in the reference configuration is given by:

$$\boldsymbol{\phi}_c = \left(\frac{\partial^2 \Psi_c}{\partial \mathbf{E}_c \partial \mathbf{E}_c} \right)^{-1} : \left[\sum_{c=1}^{n} k_c \left(\frac{\partial^2 \Psi_c}{\partial \mathbf{E}_c \partial \mathbf{E}_c} \right)^{-1} \right]^{-1} \tag{6}$$

where $\left(\frac{\partial^2 \Psi_c}{\partial \mathbf{E}_c \partial \mathbf{E}_c} \right)^{-1}$ is the constitutive tensor of the c–th component and

$\left[\sum_{c=1}^{n} k_c \left(\frac{\partial^2 \Psi_c}{\partial \mathbf{E}_c \partial \mathbf{E}_c} \right)^{-1} \right]^{-1}$ is the composite serial constitutive tensor, both referred to the reference configuration.

The fourth order tensor $\boldsymbol{\phi}_c$ provides the mapping between the strains to its serial counterpart in the reference configuration ensuring the serial equilibrium constraint.

The second Piola-Kirchhoff stress tensor can be obtained using Eq. 4 as follows

$$\mathbf{S} = m\frac{\partial \Psi}{\partial \mathbf{E}} = \sum_{c=1}^{n} k_c m_c \frac{\partial \Psi_c}{\partial \mathbf{E}_c} \frac{\partial \mathbf{E}_c}{\partial \mathbf{E}} = \sum_{c=1}^{n} k_c \mathbf{S}_c \frac{\partial \mathbf{E}_c}{\partial \mathbf{E}} \tag{7}$$

For the further application should be useful to write the Cauchy stress throughout a push over operation

$$\boldsymbol{\sigma} = \frac{1}{J}\mathbf{F} : \mathbf{S} : \mathbf{F}^T \tag{8}$$

where $\mathbf{F}$ is the deformation gradient.

2.3 Constitutive model for each component of the composite material: anisotropic component model

The anisotropic model used in this work is based on the assumption that each kinematic configuration is split in two spaces (Oller et al. 2003); a real anisotropic space and a fictitious isotropic one (see Fig. 1). The problem is solved in the fictitious isotropic space allowing the use of constitutive models originally developed for isotropic materials. The anisotropic behavior of the material is expressed in terms of isotropic fictitious stress and strain spaces, which are the linear tensor transformations of the real anisotropic stress and strain spaces. All the information on the material anisotropy is contained in the fourth order transformation tensors A^s and A^E in the reference configuration relating the stresses and strains in the real (anisotropic) and fictitious (isotropic) spaces (see Appendix A for derivation details).
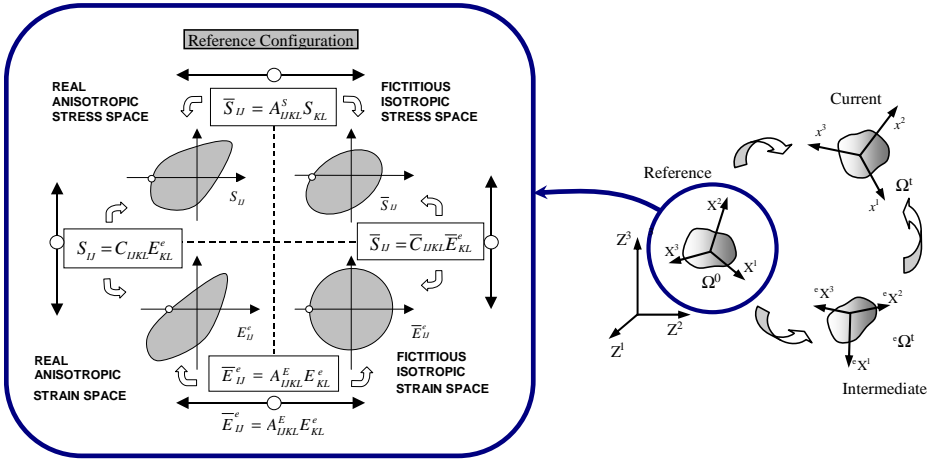

Figure 1: Schematic view of the "Kinematic Configurations" and its split on "Anisotropic Stress and Strain Spaces"

The transformation of the second Piola – Kirchhoff stress tensor S in the anisotropic space to the isotropic space is performed by:

$$\bar{\mathbf{S}} = \mathbf{A}^s \mathbf{S} \tag{9}$$

where $\mathbf{A}^s$ is a fourth order tensor which relates the stress tensors in the real and fictitious spaces, $\bar{\mathbf{S}}$ and $\mathbf{S}$ are the second Piola–Kirchhoff stress tensor in the fictitious isotropic and real anisotropic stress spaces respectively.

The fourth order tensor $\mathbf{A}^s$ is defined in the reference configuration and remains constant in it. It is also necessary to define the relationship between the Green–Lagrange elastic strain in the real anisotropic space $\mathbf{E}$ and the Green–Lagrange elastic strain $\bar{\mathbf{E}}$ in the fictitious isotropic space. This relation is

$$\bar{\mathbf{E}} = \mathbf{A}^E \mathbf{E} \tag{10}$$

The strain transformation tensor is computed taking into account Eqs. (9) and (10).

$$\mathbf{A}^E = \bar{\mathbf{C}}^{-1} \mathbf{A}^S \mathbf{C} \tag{11}$$

where $\bar{\mathbf{C}}$ is the constitutive tensor in the isotropic space and $\mathbf{C}$ is the constitutive tensor in the real anisotropic space. The choice of $\bar{\mathbf{C}}$ can be arbitrary and for this purpose the properties of any known material can be chosen, because their influence in the computations is cancelled when all the quantities are returned to the real space.

3   Constitutive growth/atrophy model for a material component considering biological availability

In previous sections the formulation of a new general mixing theory for the mechanical treatment of biological composite material, through the behavior of their single components, has been presented. Also, a general formulation for the treatment of the anisotropy of each material component, based on an isotropic formulation, was introduced. In this section a new constitutive law that governs the mechanical-biological growth for each material component of the tissue is proposed.

Tissue growth also occurs under certain pathological conditions like vascular and cardiac hypertrophy, manifested by increased stresses in the walls of the tissues (Humphrey 2002).

It is now well established through previous works (Skalak et al. 1996, Rodriguez et al. 1994), that growth and remodeling produce incompatible strains. For example, if the growth of some cells compress others, elastic stresses are developed which tend to eliminate gaps and avoid overlap between them. For this reason, Fung (1981) proposed that both cardiac hypertrophy and normal growth are developed in response to increased hemodynamic load, altering both systolic and diastolic heart walls. The same situation occurs in bone tissue where the osteocytes motivate the cell development due to its sensitivity to applied stresses (Baiotto and Zidi, 2004).

There are several proposed laws for the growth of bones based on mechanical stimulus. In that sense, Fung (1996) proposed that the tissue growth depends on the stresses acting on them. In this formulation, growth/atrophy of parts of the tissue occurs so that the stresses reach a steady state:

If the stresses exceed the threshold homeostatic equilibrium, the tissue growth and these stresses are relaxed to meet this condition.

If the stress is below the current threshold homeostatic equilibrium, reabsorption or atrophy occurs in the tissue to achieve equilibrium.

3.1 Governing equations

The formulation proposed in this article derives from the works by Rodriguez et al (1994), Lubarda and Hoger (2002) and Himpel et al (2005). Growth is considered by means of a multiplicative decomposition of the deformation gradient F. The kinematics in finite strains is expressed in its simplest form (Lubarda and Hoger 2002), as:

$$\mathbf{F} = \mathbf{F}^{ev}\mathbf{F}^g \tag{12}$$

where $\mathbf{F}^{ev}$ is the elastic-viscous part and F^g is the incompatible part, which includes "growth/atrophy" phenomena. The total volume change can be written as $dv = JdV = (J^{ev}J^g)dV$, where $J = \det\mathbf{F}$, $J^{ev} = \det\mathbf{F}^{ev}$ and $J^g = \det\mathbf{F}^g$.

The previously described kinematics is also accompanied by the following change of mass,

$$dm = \rho\,dv = \rho_0^{ini}\,dV + \left[\int_t R_0\,dt\right]dV \Rightarrow \rho_0 = \rho_0^{ini} + \int_t R_0\,dt \tag{13}$$

where ρ_0^{ini} and ρ_0 represent the density in the reference configuration at the beginning of the process and at any moment of it, ρ is the density in the current configuration, dm and dv are the mass and volume differentials in the current configuration and R_0 the source of mass in the reference configuration.

In the cases of growth or atrophy there is a mass change and the density in the current configuration ρ remains practically constant. Furthermore, the relations between the different densities are given by

$$\rho_0 = \rho J = \rho_0^{ini} J^g \tag{14}$$

This mass change at constant density requires a volume change leading to a new mass balance, namely

$$\dot{\rho}_0^{ini} = 0 \Rightarrow \dot{\rho}_0 = \rho_0^{ini}\dot{J}^g = R_0 \tag{15}$$

and hence the following definition of the source of mass,

$$R_0 = \rho_0\,\mathrm{tr}\hat{\mathbf{L}}^g = J^g\,\rho_0^{ini}\,\mathrm{tr}\hat{\mathbf{L}}^g = J^g\,\rho_0^{ini}\,\mathrm{tr}\left(\dot{\mathbf{F}}^g \cdot \mathbf{F}^{g^{-1}}\right) \tag{16}$$

where $\hat{\mathbf{L}}^g$ is the velocity growth gradient. Thus, if the strain growth gradient $\mathbf{F}^g$ and its temporal evolution are known, the source of mass is immediately known.

For the mechanical treatment of the tissue an elastic-viscous potential $W(\hat{\mathbf{C}}, \Gamma^v)$ is defined, where $\hat{\mathbf{C}} = \mathbf{F}^{ev^T} \cdot \mathbf{F}^{ev}$ is the right elastic-viscous Cauchy tensor, Γ^v is viscous variable, that in this work will not be considered. Based on this potential the following stresses are obtained

$$\hat{\mathbf{S}} = 2\rho_0 \frac{\partial W(\hat{\mathbf{C}}, \Gamma^v)}{\partial \hat{\mathbf{C}}} \; ; \; \text{with} \; \mathbf{S} = \mathbf{F}^{g^{-1}} \cdot \hat{\mathbf{S}} \cdot \mathbf{F}^{g^{-T}}; \; \text{and} \; \boldsymbol{\sigma} = \mathbf{F} \cdot \mathbf{S} \cdot \mathbf{F}^T \qquad (17)$$

where $\mathbf{S}$ and $\hat{\mathbf{S}}$ are the second Piola-Kirchhoff stress tensor in the referential and intermediate configuration, respectively .

3.2 *Isotropic growth/atrophy for each biological material component*

The isotropic growth deformation gradient is defined as (Lubarda and Hoger 2002)

$$\mathbf{F}^g = \vartheta \cdot \mathbf{I} \qquad (18)$$

where ϑ is the isotropic growth stretch.

The rate of growth can be expressed as:

$$\hat{\mathbf{L}}^g = \dot{\mathbf{F}}^g \cdot \mathbf{F}^{g^{-1}} = \frac{\dot{\vartheta}}{\vartheta} \mathbf{I} \qquad (19)$$

During the growth process the density is conserved. Taking into account Eq. 19 the mass source from Eq. 16 results,

$$R_0 = 3 \, \vartheta^2 \, \rho_0^{\text{ini}} \, \dot{\vartheta} \qquad (20)$$

For a certain range of stresses there is a homeostatic equilibrium without mass change. In this state new cells are produced only to replace those that die, so mass and volume remain constant. This equilibrium state is defined by an upper limit $\boldsymbol{\sigma}_{eq}^{*+}$ and a lower one $\boldsymbol{\sigma}_{eq}^{*-}$. For stresses higher than the upper limit a mechanical stimulus growth zone is defined. The lower limit corresponds to the start of the atrophy zone. In this work the trace of the Cauchy stress tensor is proposed to characterize the mechanical state of stress and consequently the evolution rule of ϑ. This choice is made to allow a more straightforward definition of the limits of growth and atrophy zones, because of the values of stress from experimental results are usually given in the current configuration.

A simple mechanical stimulus generation is not enough to produce a mass increase, but it is necessary that the metabolism is able to allow tissue growth. For this

purpose the necessary nutrients, enzymes etc. must be available. Hence the amount of tissue growth that the metabolism can sustain with the available nutrients will be regarded as "bioavailability" for growth.

To this end a new variable to take into account the biological availability for growth θ, is proposed.

Following these considerations the evolution rule proposed is expressed as:

$$\dot{\vartheta} = g(tr\boldsymbol{\sigma}, \boldsymbol{\sigma}_{eq}^*)\, f(\theta, \vartheta) \tag{21}$$

where $g(tr\boldsymbol{\sigma}, \boldsymbol{\sigma}_{eq}^*)$ determinates the growth/atrophy rate as a function of the Cauchy stress, $f(\theta, \vartheta)$ is a function that regulates the metabolic part of the growth phenomena and allows, or not, growth according with biological availability to generate new tissue, and it is developed in detail in the next section.

If an unlimited source of nutrients is considered, the growth rate is limited by the rate at which cell division and collagen recruitment occur in that particular tissue. This rate limit is considered by mean of the maximum rate of mass production $M_{\max}$ expressed as the percentage of the initial mass that can be produced in a unit of time when the only limitation is the cell division and collagen recruitment rate. Therefore, the maximum growth stretch rate is

$$\dot{\vartheta} = \frac{M_{\max}}{3\,\vartheta^2} \tag{22}$$

In the case of atrophy the rate at which the tissue can be reabsorbed defines the rate of mass decrease. The limit values for growth and atrophy are named $\dot{\vartheta}_{MAX}^+$ and $\dot{\vartheta}_{MAX}^-$ respectively. In the atrophy and growing zones linear relationships (with k^+ and k^- slopes) are adopted. Finally, the resulting growth-stimulus function is depicted in Fig. 2. Its general form is similar to that proposed by Rodriguez et al (2006), where three main zones can be observed.

The expression of the function of mechanical stimulus for each zone in Fig. 2 is:

$$\begin{cases} g(tr\boldsymbol{\sigma}, \boldsymbol{\sigma}_{eq}^*) = k^+\,(tr\boldsymbol{\sigma} - \boldsymbol{\sigma}_{eq}^{*+}) & \text{If } (tr\boldsymbol{\sigma} - \boldsymbol{\sigma}_{eq}^{*+}) > 0 \\ g(tr\boldsymbol{\sigma}, \boldsymbol{\sigma}_{eq}^*) = 0 & \text{If } \boldsymbol{\sigma}_{eq}^{*+} > tr\boldsymbol{\sigma} > \boldsymbol{\sigma}_{eq}^{*-} \\ g(tr\boldsymbol{\sigma}, \boldsymbol{\sigma}_{eq}^*) = k^-\,(tr\boldsymbol{\sigma} - \boldsymbol{\sigma}_{eq}^{*-}) & \text{If } (tr\boldsymbol{\sigma} - \boldsymbol{\sigma}_{eq}^{*-}) < 0 \end{cases} \tag{23}$$

The formulation to represent the effect of the biological availability is developed in the next section.

3.3 *Biological growth availability for each biological material component*

Stress driven growth/atrophy is based on the concept of adding or removing mass motivated by a mechanical stimulus. During this process, incompatible strains are developed. These strains are related with the growth part of the stress gradient $\mathbf{F}^g$.
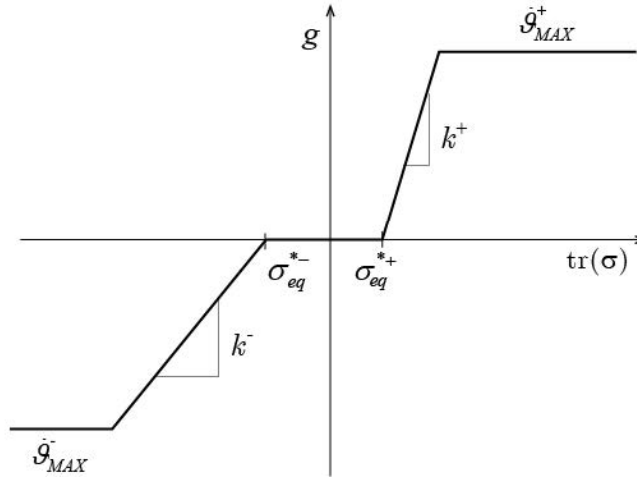
Figure 2: General form of the mechanical growth-stimulus function

The biological availability concept works as an activation law. Growth will only take place if the metabolism of the cells is capable of generating new tissue and a growth mechanical stimulus is present. When we refer to biological availability it must be understood that all the elements necessary for growth (proteins, enzymes, growth factors, etc.) are present. We will refer to these elements as "nutrients" from now on.

A variable of biological availability for growth θ is introduced. This variable is responsible of the activation of the mass change and represents the mass production that the metabolism can sustain with the available nutrients.

The availability of nutrients in a given time is obtained by a balance between incorporated nutrients and those used for growing tissue. In this work the amount of nutrients entering the system is taken into account by the function $N^i(t)$. It considers an initial reserve of nutrients R_i and a discrete contribution of nutrients A_t at regular time intervals. The values of $N^i(t)$ are dimensionless and represent the mass increment of nutrients referred to the initial mass of the system. For instance a value of $N^i = 1.02$ represents the entry to the system of nutrients enough to generate an increase of tissue mass of 2% respect to its original mass. Fig. 3 shows the function of nutrients contribution.

The biological availability internal variable proposed results from the balance be-
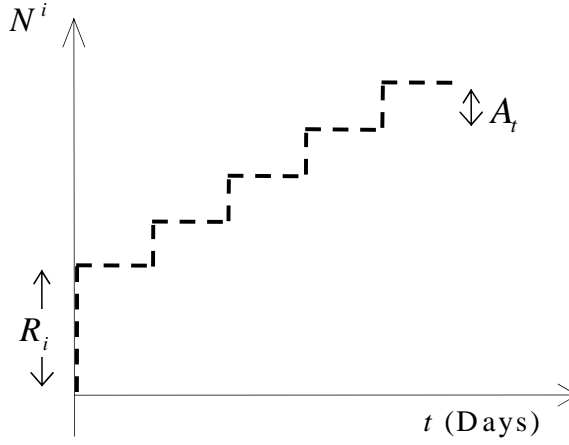
Figure 3: Nutrients entering the system

tween the nutrients contributed to the system and those consumed in tissue growth:

$$\theta(t) = N^i(t) - \det[\mathbf{F}^g(t)]\frac{\rho_0}{\rho_t} \qquad (24)$$

During growth phenomena density remains constant $\rho_0 = \rho_t$.

Biological availability will increase whenever the rate of nutrients contribution is greater than the growing rate. However, there is a physical limit to the amount of nutrients the system can keep in reserve. Consequently, an upper boundary for the biological availability $\theta^{\max}$ is incorporated in the formulation.

Finally, the following definition of the biological availability function $f(\theta, \vartheta)$ is proposed:

$$f(\theta, \vartheta) = \begin{cases} 1 & \text{if } g(tr\boldsymbol{\sigma}, \boldsymbol{\sigma}^*_{eq}) \leq \frac{\dot{\theta}}{3\,\vartheta^2} \\[2ex] \frac{\left(\frac{\dot{\theta}}{3\,\vartheta^2}\right)}{g(tr\boldsymbol{\sigma}, \boldsymbol{\sigma}^*_{eq})} & \text{if} \quad g(tr\boldsymbol{\sigma}, \boldsymbol{\sigma}^*_{eq}) > \frac{\dot{\theta}}{3\,\vartheta^2} \end{cases} \qquad (25)$$

3.3.1 Numerical implementation of a constitutive growth for a single biological component material

The proposed formulation has been implemented in a finite element code. The isotropic growth stretch ϑ given by Eq. 18, is treated as an internal variable written in an incremental way as follows:

$$\Delta\vartheta = \dot{\vartheta}\,\Delta t \;\; \Rightarrow \;\; \mathfrak{R}_\vartheta = -\Delta\vartheta + \left[g(tr\boldsymbol{\sigma}, \boldsymbol{\sigma}^*_{eq})\, f(\theta)\right]\Delta t \qquad (26)$$

The solution is achieved minimizing the residue using a Newton-Raphson scheme

$$\mathfrak{R}_{\vartheta}^{k+1} = \mathfrak{R}_{\vartheta}^{k} - \Delta\vartheta + \frac{\partial\dot{\vartheta}}{\partial\vartheta}\Delta\vartheta\,\Delta t = 0 \tag{27}$$

$$\Delta\vartheta = \left(1 - \frac{\partial\dot{\vartheta}}{\partial\vartheta}\Delta t\right)^{-1}\mathfrak{R}_{\vartheta}^{k} \ \Rightarrow\ \vartheta^{k+1} = \vartheta^{k} + \Delta\vartheta \tag{28}$$

The proposed algorithm for growth/atrophy is resumed as in Box 1.

4   Representative numerical simulations

4.1   *Growth under uniaxial stress*

To show the capabilities of the mechanical model presented in the previous sections, an uniaxial stretching test on a single hexahedral finite element is carried out in this section. Fig. 4 shows the element, its boundary conditions and the prescribed uniaxial stretching.

To illustrate the anisotropic behavior of the tissue, two stretch directions are considered ($\alpha = 0^o$, $\alpha = 20^o$), being α the angle between the mean fibers direction and the stretch direction. The tissue is modeled considering a matrix reinforced by a single family of collagen fibers. A mixed pressure - displacement finite element formulation (Crisfield 1997), has been used in this work to avoid locking and instability issues arising from tissue incompressibility.

The details regarding the calibration of the serial-parallel parameter are depicted in Appendix B. For the sake of simplicity, an incompressible Neo Hook model is chosen with C_m =6.796 kPa (for the matrix) and C_f =348.2 kPa (for the fibers). The participation ratios for matrix and fiber are chosen as $k_m = 0.80$ and $k_f = 0.20$, respectively. The maximum mass production rate adopted is $R_{\max}^{=}1.13\%$ day, extrapolated from studies of stress-induced changes of the arterial wall thickness in response to hypertension in rats (Fridez et al. 2003). Growth upper limit σ_{eq}^{*+} is adopted as 6.5 kPa and $k^+ = 0.001$.

Biological availability is limited by an initial reserve of $R_i = 3\%$ and a discrete contribution $A_{0.5} = 0.30\%$ each half day.

The element is stretched in one step and the stretch of $\lambda_x = 1.075$ is kept constant for 40 days. The initial value of the Cauchy stress tensor trace of the tissue is 33.62 kPa for $\alpha = 0^o$ and 11.63 kPa for $\alpha = 20^o$. The difference between both values reflects the fact the fibers must be aligned with the stretch direction in order to fully contribute their strength. These values are higher than the growth stimulus boundary and, consequently, the growth stretch value increases as can be seen in Fig. 5c.

<div align="center">Box 1: Proposed algorithm</div>

---

1. Initialize variables with previous step values.

$$\boldsymbol{F}^{ev} = \boldsymbol{F} \cdot \boldsymbol{F}^{g^{-1}}\Big|_n \quad \Rightarrow \quad \hat{\boldsymbol{C}} = \boldsymbol{F}^{evT} \cdot \boldsymbol{F}^{ev} \Rightarrow \quad \hat{\boldsymbol{S}} = 2\frac{\partial \Psi}{\partial \hat{\boldsymbol{C}}} \Rightarrow \quad \boldsymbol{S} = \boldsymbol{F}^{g^{-1}} \cdot \boldsymbol{S} \cdot \boldsymbol{F}^{g^{-T}}$$

$$\Rightarrow \quad \boldsymbol{\sigma} = \boldsymbol{F} \cdot \boldsymbol{S} \cdot \boldsymbol{F}^T \ ; \qquad \rho_0 = \rho_{0n} \quad ; \qquad \vartheta = \vartheta_n$$

2. Control of growth/atrophy condition.

if $\ tr\sigma \geq \sigma_{eq}^{*+}\ $ then (Growth)

$$g(tr\sigma, \sigma_{eq}^*) = \begin{cases} k^+ \,(tr\sigma - \sigma_{eq}^{*+}) & \text{if} \quad k^+ \,(tr\sigma - \sigma_{eq}^{*+}) \leq \dot{\vartheta}_{MAX}^+ \\ \dot{\vartheta}_{MAX}^+ & \text{if} \quad k^+ \,(tr\sigma - \sigma_{eq}^{*+}) > \dot{\vartheta}_{MAX}^+ \end{cases}$$

if $\ \Rightarrow \left(k^+ \,(tr\sigma - \sigma_{eq}^{*+})\,\Delta t \right) < \sqrt[3]{\theta} \ \Rightarrow f(\theta,\vartheta) = 1 \ \Rightarrow \ \dot{\vartheta} = k^+(tr\sigma - \sigma_{eq}^{*+})$

else $\qquad f\left(\theta,\vartheta\right) = \dfrac{\left(\dfrac{\dot{\theta}}{3\,\vartheta^2}\right)}{g(tr\sigma, \sigma_{eq}^*)} \quad \Rightarrow \quad \dot{\vartheta}_{\max} = \dfrac{M_{\max}}{3\,\vartheta^2}$

elseif $\ tr\sigma < \sigma_{eq}^{*-}\ $ then (Atrophy)

$$g(tr\sigma, \sigma_{eq}^*) = \begin{cases} k^- \,(tr\sigma - \sigma_{eq}^{*-}) & \text{if} \quad k^- \,(tr\sigma - \sigma_{eq}^{*-}) \geq \dot{\vartheta}_{MAX}^- \\ \dot{\vartheta}_{MAX}^- & \text{if} \quad k^- \,(tr\sigma - \sigma_{eq}^{*-}) < \dot{\vartheta}_{MAX}^- \end{cases}$$

$$\dot{\vartheta} = k^- \,(tr\sigma - \sigma_{eq}^{*-})$$

Else

$\dot{\vartheta} = 0$ (Homeostatic equilibrium) $\quad \rightarrow \quad$ **Go To 4**

3. Newton-Raphson solution of growth/atrophy problem.

3.1 Growth/atrophy residue.

$$\Re_{\vartheta} = -\Delta\vartheta + \left[\, g(tr\sigma, \sigma_{eq}^*) \ f(\theta) \right] \Delta t$$

3.2 Tolerance control.

if $\ \left\| \Re_{\vartheta} \right\| \leq \ $ Tol $\qquad$ **Go To 4**

3.3 Density and growth/atrophy stretch update:

$$\Delta\vartheta = \left(1 - \frac{\partial \dot{\vartheta}}{\partial \vartheta}\Delta t\right)^{-1} \Re_{\vartheta}^k \ \Rightarrow \ \vartheta^{k+1} = \vartheta^k + \Delta\vartheta \Rightarrow \rho_0 = \vartheta^3 \rho^{ini}$$

3.4 Checks biological availability for growth.

if $\quad J^g \Big|_{n+1}^{k+1} - J^g \Big|_n < \theta \Rightarrow \vartheta^{k+1} = \vartheta^{k+1}$

else $\quad \Rightarrow \vartheta^{k+1} = \sqrt[3]{\theta}$

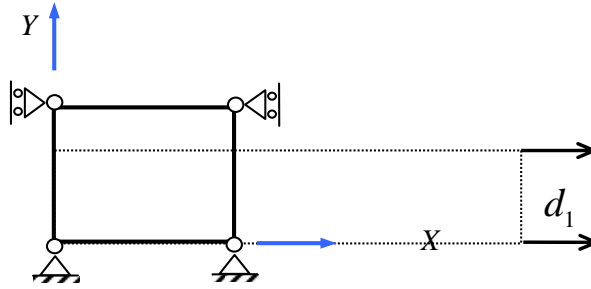*3.5 Update of growth stretch and Cauchy stresses* $\rightarrow \quad$ Go To 3.1

4   EXIT
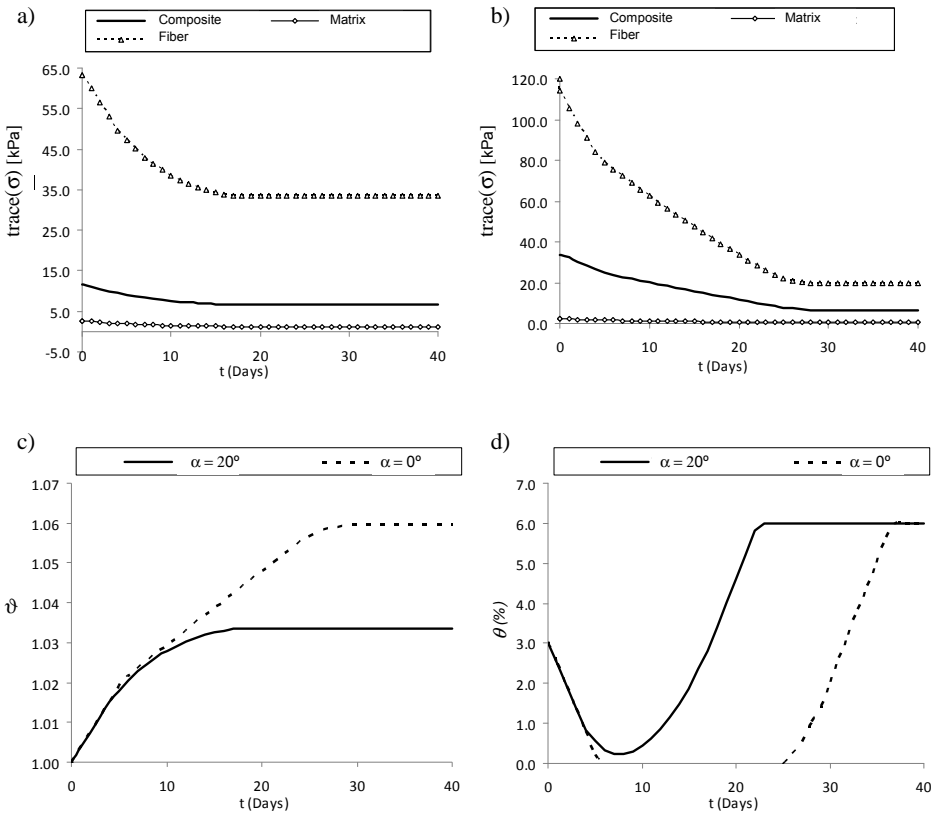
Figure 4: Boundary conditions and prescribed displacements

Figure 5: a) Evolution of Cauchy stress trace for $\alpha = 20^{o}$. b) Evolution of Cauchy stress trace for $\alpha = 0^{o}$ c) Growth stretch. d) Biological availability for growth θ.

When the tissue grows the growth part of the deformation gradient increases, while the elastic part decreases and the stress relaxes (Fig. 5a and 5b).

The stress contributions of the tissue components for $\alpha = 20^o$ and $\alpha = 0^o$ are plotted in Fig. 5a and 5b, respectively. In both cases the fiber contributes with most of the tissue strength. Fiber contribution to the tissue strength depends fundamentally on its orientation as can be noticed comparing Figures 5a and 5b.

For the first 7 days the growth rate is similar for both cases ($\alpha = 20^o$, $\alpha = 0^o$) because it is sustained mainly by the initial reserve, growth rate is then controlled by the maximum growth rate. For $\alpha = 20^o$ the stress relaxes due to growth until equilibrium is found at day 17, when the Cauchy stress trace reaches the growth upper limit σ_{eq}^{*+} the stress imbalance is null and growth stops, as can be seen in Fig. 5c. The biological availability decreases steeply during the first six days, given the high grow rate. In this lapse the nutrients that entered the system and the initial reserve are nearly depleted. Between days six and ten the nutrient intake and consumption due to growth are almost matched reaching a minimum in day 8. After this time the mechanical stimulus diminished to a level at which the growth rate is smaller than the rate of nutrients intake and, consequently, the biological availability increases showing a steeper slope as growth rate diminishes due to lack of mechanical stimulus. The biological availability function increases until the prescribed limit $\theta^{\max}$ is reached. For this case there are nutrients available during al all times and consequently growth is controlled by the mechanical stimulus.

For the case $\alpha = 0^o$ the stress is much higher and from day 7 the nutrients reserve has been completely depleted and the growth rate is controlled by the daily nutrients intake until day 25, this can be noted in Fig 5c as a change in the growth stretch curve slope. During growth the stresses relaxes and the mechanical stimulus diminishes until the Cauchy stress trace reaches the Growth upper limit σ_{eq}^{*+} at day 27.

4.2 *Notched patch under tension with unequal nutrients intake distribution*

To asses the effect of an unequal distribution of the biological availability, a variable profile of R_i and $A_{0.5}$ is prescribed along a notched patch as shown in Fig. 7a. The patch dimensions are 30mm long, 20mm wide and 1mm thick. The general patch response and, particularly, the behaviors of four reference points located symmetrically along the middle section of the patch (Fig. 6b) are considered.

The material properties and maximum mass production rate are the same as in section 4.1, σ_{eq}^{*+} is adopted as 1.90 kPa and $k^+ = 0.03$. A displacement of 1.5mm is applied instantly in the upper side. The evolution of the Cauchy stress trace and growth stretch in the patch are shown in Fig. 7 and its values for the reference
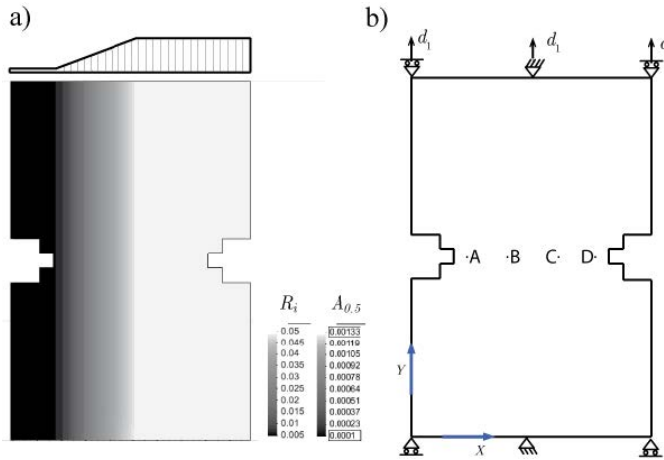
Figure 6: a) Nutrient intake distribution along the patch. b) Boundary conditions, prescribed displacements and reference points.
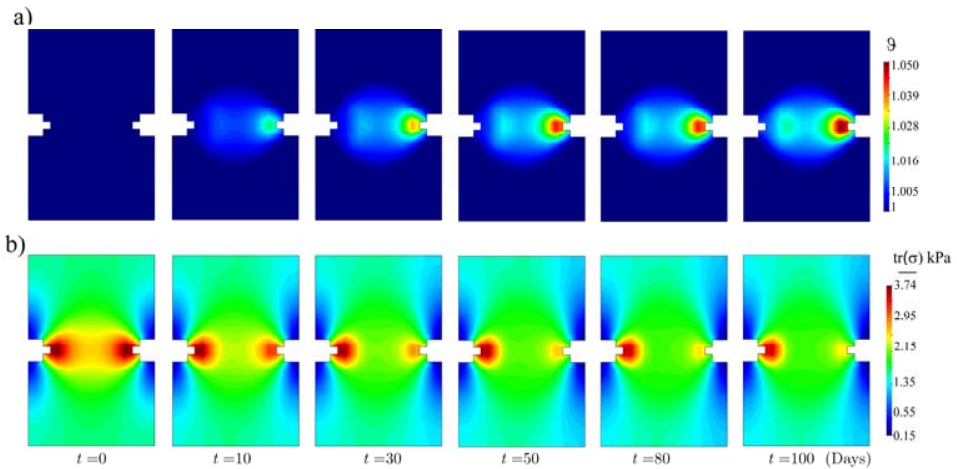

Figure 7: a) Growth stretch evolution b) Cauchy stress trace evolution during growth.

points along the middle section are plotted in Fig. 8.

As expected, the initial stress field is symmetric and the mechanical stimulus is similar in both sides of the patch. However, the unequal distribution of nutrients intake limits the growth rate of the left side of the patch as can be seen in Fig. 7a. As a consequence only the right side of the patch is able to achieve a noticeable
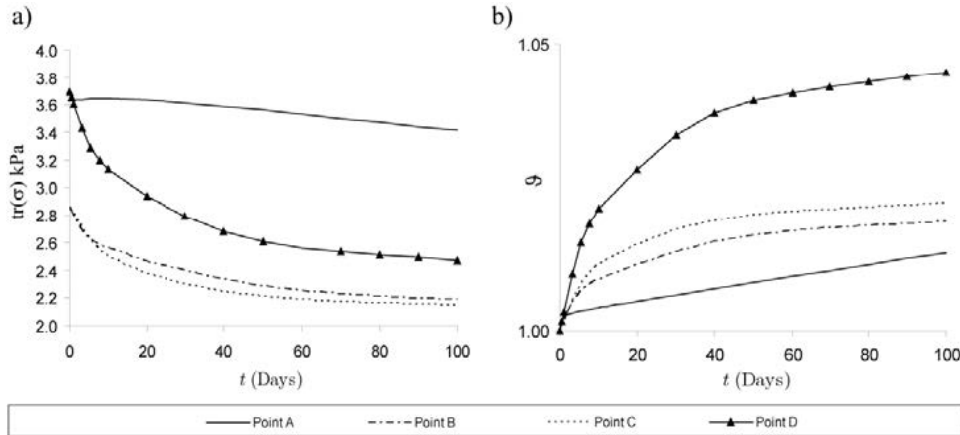
Figure 8: a) Cauchy stress trace for reference points A, B, C, D. b) Growth stretch evolution for reference points A, B, C, D.

relaxation of stresses (Fig. 7b).

Due to natural or pathological processes, tissues are not always fully able to react to mechanical stimulus. This example illustrates the ability of the proposed model to consider this possibility.

5   Conclusions

The numerical model presented here is not just a single constitutive model, but is a manager of the orthotropic constitutive models belonging to the simple materials that make up the composite (general mixing formulation, described in Section 2). The orthotropy of each single material component is approached by a general anisotropic formulation (anisotropic space mapping formulation, described in Section 3.1), which acts on a biomechanical isotropic constitutive model formulated in the isotropic space —hosted in the reference kinematic configuration— of each material component (Section 3.2). The use of all these formulations offers a great capability for the numerical simulation of mechanical and metabolic growth of the biological tissues. The main advantage of this approach is the possibility to consider different behaviors and also to obtain the mean stress and strain field of each material component of the whole biological composite material.

The anisotropy of the tissue can be considered by means of a space transformation technique, allowing the solution of the constitutive problem in a fictitious isotropic space using isotropic constitutive relationships.

A model for growth of soft tissues accounting for biological availability is pro-

posed in this work. Growth stimulus is defined as a function of the stress field, however this stimulus generation is not enough to produce growth in the tissue, it is also necessary that the metabolism allows the tissue to grow. For this reason the concept of biological availability is introduced as a limit in the mass source. This limit takes into account that metabolism requires a series of elements to sustain the growth process. All these elements are considered in a simplified way as nutrients. An internal scalar variable θ is proposed to account for the mentioned biological availability.

In the numerical implementation the nutrients entering the system are simulated in a simplified way by a temporal function parameterized at each integration point level. In future works an implementation based on the solution of a coupled mass transport field will be developed.

References

Baiotto S., Zidi M. (2004). Theoretical and numerical study of a bone remodeling model: The effect of osteocyte cells distribution. *Biomechanics and Modeling in Mechanobiology*. Issue: Volume 3, Number 1, Springer-Verlag, Sep. pp. 6–16.

Bellomo F.J., Armero F., Nallim L.G., Oller S. (2011). A constitutive model for tissue adaptation: necrosis and stress driven growth. *Mechanics Research Communications. Special issue: Biomechanics.* In Press

Car E., Oller S., Oñate E. (2000). An Anisotropic Elasto Plastic Constitutive Model for Large Strain Analysis of Fiber Reinforced Composite Materials. *Computer Methods in Applied Mechanics and Engineering.*Vol. 185, No. 2-4, pp. 245-277.

Car E., Oller S., Oñate E. (2001). A Large Strain Plasticity for Anisotropic Materials: Composite Material Application. *International Journal of Plasticity.* Vol.17, No. 11, pp. 1437-1463.

Crisfield M. A. (1997) *Nonlinear Finite Element Analysis of Solids and Structures*, Vols I, II, Wiley.

Cowin S. C. (1996).Strain or Deformation Rate Dependent Finite Growth in Soft Tissues. *J. Biomechanics*, Vol. 29, No. 5, pp. 64-649.

Cowin S. C., Hegedus D. H. (1976).Bone Remodeling I: Theory of Adaptive Elasticity. *Journal of Elasticity*, Vol. 6, No. 3, July 1976.

Epstein M., Maugin G. A. (2000).Thermomechanics of Volumetric Growth in Uniform Bodies. *International Journal of Plasticity* 16: 951-978.

Fridez, P., Zulliger, M., Bobard, F., Montorzi, G., Miyazaki, H., Hayashi, K., Stergiopulos, N. (2003). Geometrical, functional, and histomorphometric adaptation of rat carotic artery in induced hypertension. *Journal of Biomechanics* 36, 671–680.

Fung, Y. C. B. (1996). *Biomechanics*. Springer.

Fung, Y. C. B. (1981). *Biomechanics: Mechanical Properties of Living Tissues*. Springer-Verlag, New York.

Gasser T.C., Holzapfel G.A. (2002).A rate-independent elastoplastic constitutive model for (biological) fiber-reinforced composites at finite strains: Continuum basis, algorithmic formulation and finite element implementation. *Biomech Preprint Series*. Paper No. 25.

Himpel G., Kuhl E., Menzel A., Steinmann P. (2005).Computational Modelling of Isotropic Multiplicative Growth. *CMES: Computer Modeling in Engineering and Sciences*, Vol.8 No.2, pp. 119-134.

Holzapfel G. A., Ogden R. W. (2003). Biomechanics of Soft Tissue in Cardiovascular Systems. Published by Springer-Verlag Wien New York. (CISM International Centre for Mechanical Sciences. *Courses and Lectures*, No. 441. UDINE).

Humphrey, J. D. (2002).*Cardiovascular Solid Mechanics, Cells, Tissues and Organs*. Springer.

Lubarda V.A., Hoger A. (2002).On The Mechanics of Solids with a Growing Mass. *International Journal of Solids and Structures* 39; 4627–4664.

Martinez X., Rastellini F., Flores F., Oller S., Oñate E. (2011). Computationally optimized formulation for the simulation of Composite materials and delamination failures. *Composites Part B: Engineering*. Vol. 42 pp. 134–144.

Oller S., Car E., Lubliner J. (2003). Definition of a general implicit orthotropic yield criterion. *Computer Methods in Applied Mechanics and Engineering*.Vol. 192, No. 7-8, pp. 895-912.

Rastellini F., Oller S., Salomón O. and Oñate E. (2008). Composite material non-linear modelling for long fibre-reinforced laminates. Continuum basis, computational aspects and validations. *Computers and Structures Vol.* 86, pp. 879-896.

Rodriguez E., Hoger A. and McCulloch A.D. (1994).Stress-Dependent Finite Growth in Soft Elastic Tissues. *J. Biomechanics*, Vol. 21, No. 4, Pp. 455-467

Skalak R., Zargaryan S., Jain R. K., Netti P. A., Hoger A. (1996).Compatibility and the genesis of residual stress by volumetric growth. *J. Math. Biol*. Vol. 34, pp. 889–914.

APPENDIX A: definition of the transformation tensors.

There are several ways of defining the transformation tensor $\mathbf{A}^S$, examples of which can be seen in the work of Betten (1981), Oller *et al.* (1995, 1996, 1998), Car *et al.* (2000,2001), Oller *et al.* (2003), and others. Although with these definitions it is possible to find adequate orthotropic yield criteria, it is difficult to adjust them "exactly" to represent desired material behavior. In order to circumvent this limitation its can be seen an exact definition for $\mathbf{A}^S$ in Oller *et al.* (2003). Here in what follows a most simple definition of the tensor $\mathbf{A}^S$ will be introduced. This is achieved by means of the following relation:

$$\left(\mathrm{A}^S_{ijkl}\right)^{-1} \equiv W_{ijkl} \tag{A.1}$$

where $W_{ijkl} = \omega_{ik}\omega_{jl}$ contains information on the yield stresses along every axis of orthotropy (f_x, f_y, f_z, with $f_i = \sqrt{f_i^t f_i^c}$) and conventional isotropic yield stress ($f = \sqrt{f^t f^c}$), with $\omega_{ij} = \mathrm{Diag}\left\{\omega_{\{xx\}}; \omega_{\{yy\}}; \omega_{\{zz\}}\right\} = \mathrm{Diag}\left\{\sqrt{f_x/f}; \sqrt{f_y/f}; \sqrt{f_z/f}\right\}$, such that, with the help of the symmetries of the tensor W_{ijkl}, the following matrix form is obtained:

$$W_{ijkl} = \omega_{ik}\omega_{jl} =$$

$$\begin{bmatrix} \omega_{\{xx\}}\omega_{\{xx\}} & 0 & 0 & 0 & 0 & 0 \\ 0 & \omega_{\{yy\}}\omega_{\{yy\}} & 0 & 0 & 0 & 0 \\ 0 & 0 & \omega_{\{zz\}}\omega_{\{zz\}} & 0 & 0 & 0 \\ 0 & 0 & 0 & \omega_{\{xx\}}\omega_{\{yy\}} & 0 & 0 \\ 0 & 0 & 0 & 0 & \omega_{\{yy\}}\omega_{\{zz\}} & 0 \\ 0 & 0 & 0 & 0 & 0 & \omega_{\{zz\}}\omega_{\{xx\}} \end{bmatrix} \rightarrow$$

$$\xrightarrow{\text{In Matrix form}} W_{IJ} = \omega_{ii}\omega_{jj} = \begin{bmatrix} \omega_{11} & 0 & 0 & 0 & 0 & 0 \\ 0 & \omega_{22} & 0 & 0 & 0 & 0 \\ 0 & 0 & \omega_{33} & 0 & 0 & 0 \\ 0 & 0 & 0 & \omega_{44} & 0 & 0 \\ 0 & 0 & 0 & 0 & \omega_{55} & 0 \\ 0 & 0 & 0 & 0 & 0 & \omega_{66} \end{bmatrix}$$

$$\tag{A.2}$$

The isotropic tensor $\mathbf{A}^S$ is recovered by enforcing the equality of the uniaxial yield stresses in all directions,$f_x = f_y = f_z = f$, so that the tensor $\omega_{ij} \equiv \delta_{ij}$ coincides with the Kronecker delta. This assertion is confirmed in Oller *et. al.* (2003).

APPENDIX B: Parameter Calibration for the Proposed Rule of Mixtures

The parameter χ_c is a scalar measurement of the amount of serial or parallel behaviour of the components (being $\chi_c = 0$ for complete parallel behavior and $\chi_c = 1$ for complete serial behavior). To calibrate this parameter we consider a transversally isotropic composite layer reinforced by long fibers aligned in a preferential direction α (being α the angle between the proffered fibers direction and the stretch direction) and E_θ is the elastic modulus of the composite in α direction. To address the amount of serial and parallel behaviour of a composite for different reinforcement fibers orientations, a set of numerical tests was preformed using the classical rule of mixtures and a space mapping technique ("the vanishing fiber approach", Oller 2003). As a result the contribution of one family of fibers to the load bearing capacity of the composite was obtained for different orientations. The χ_c value for the α angle is defined as:

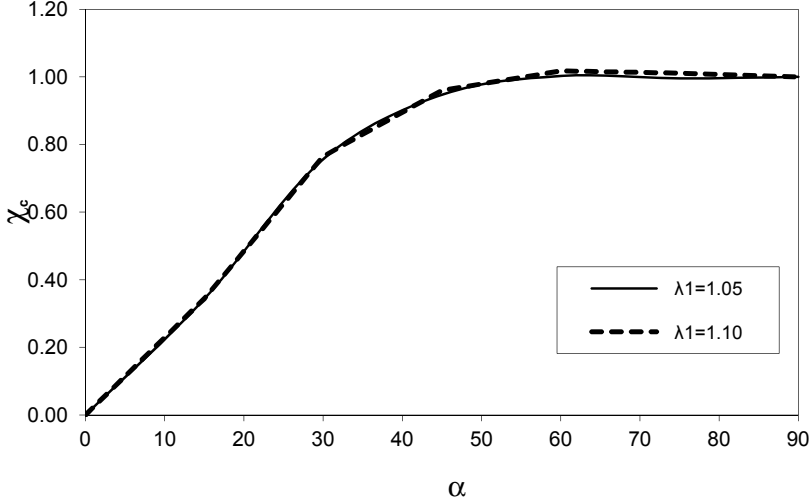$$\chi_c|_\alpha = \frac{E_{0^o} - E_\alpha}{E_{0^o} - E_{90^o}} \tag{A.3}$$

Figure 9: Variation of χ_c as a function of α angle

The tests were performed for different levels of stretch obtaining very similar values, so a unique function is adopted and the obtained values are shown in Figure B.1.